EVALUATING PLASTIC BENDING USING THE COZZONE METHOD AND MATERIAL NON-LINEAR FEA

by

MIKAELA LEEVY

Presented to the Faculty of the Honors College of

The University of Texas at Arlington in Partial Fulfillment

of the Requirements

for the Degree of

HONORS BACHELOR OF SCIENCE IN MECHANICAL ENGINEERING

THE UNIVERSITY OF TEXAS AT ARLINGTON

May 2023

ACKNOWLEDGMENTS

I would like to acknowledge my faculty mentors Dr. Kent Lawrence and Dr. Kilmain, with continued support from Dr. Raul Fernandez, for their help along with two great semesters in the senior design class. I would like to thank Dr. Brian Shonkwiler for testing the pin.

Additionally, I would like to thank my senior design team, Muid Khan, Mostapha Khazem, Jonathan Kroll, and Andrew McConnell for being a great team and for working well together. I would like to thank my Mom and Dad for all their support in college. Additionally, for my Dad's encouragement as a fellow engineer. I would also like to thank my brothers for being encouraging in my college endeavor. I would also like to thank my roommate Krishna Patel for being a great roommate and fellow engineer.

April 26, 2023

ABSTRACT

EVALUATING PLASTIC BENDING USING THE COZZONE METHOD AND MATERIAL NON-LINEAR FEA

Mikaela Leevy, B.S. Mechanical Engineering

The University of Texas at Arlington, 2023

Faculty Mentor: Raul Fernandez

In a wide range of practical applications, plastic bending analysis methods are important in understanding the structural capability of a part beyond the elastic range of a material. In the senior design project of which I am a member, a 3/8 inch diameter pin is a key structural component for a mooring cam product targeted at marine applications. The goal of this project is to compare two analysis methods of plastic bending in this pin to elastic calculations and experimental data. The two plastic analysis methods used are the Cozzone method and material non-linear finite element analysis with three-point bending boundary conditions. The Cozzone method employs an analytical technique to solve for the plastic moment, while the non-linear finite element model is solved in ANSYS software. The deflection from the non-linear finite element model is further compared to the experimental data of a three-point bending test. The results of the finite element model

and the Cozzone method show that the 1040 steel pin would fail under a max load of 3300 lb. Additionally, the finite element model did not match the experimental results.

TABLE OF CONTENTS

LIST OF ILLUSTRATIONS

LIST OF TABLES

LIST OF NOMENCLATURE

f_b - bending stress

M - moment

c - distance to neutral axis

I - moment of inertia

m_r - resisting moment of section r

m_b - resisting moment of section b

f_r - extreme fiber stress of rectangular distribution

Q - first area moment

k - shape factor

f_o - stress at neutral axis

e_u'- plastic strain

e_u - elastic strain

E - modulus of elasticity

n - Ramberg-Osgood number

F_{tu} - ultimate tensile strength

F_y - yield strength

f_m - limiting fiber stress

ε - strain

K - constant

σ - stress

τ - shear stress

V - shear force

A - area

CHAPTER 1

INTRODUCTION

1.1 Project Introduction

Mechanical devices commonly have key load bearing parts or structures that are critical to their operation. Designing the part to be structurally sound, but not overdesigned, saves material and money. Metals have a loading zone called the elastic zone where the material properties remain constant. Permanent deformation occurs when the material enters the plastic zone. Structural components are designed to remain within the elastic region for operational loading of the equipment. However, when a maximum load exceeds the elastic zone, plastic analysis determines whether a given load will exceed the ultimate strength of the material. In this honors project, plastic bending analysis is performed on a mooring cam pin to determine what happens at the maximum load.

1.2 Senior Design Project

This honors project has been pursued as an outgrowth of the Mechanical & Aerospace Engineering Department senior design course. Our senior design team was charged with designing a mooring device for boats in the Norwegian fjords. The design is based off the existing rock-climbing cam shown in Figure 1.1. The basic design of the mooring device consists of four logarithmically curved lobes that are placed into a crack and have equal friction force due to the tangent line created by the logarithmic curve. The mooring device then includes a wedge to prevent the mooring cam from "walking" or slipping out (Figure 1.2). The primary load bearing component of this device is the pin, which has a normal operating load of approximately 500 lbs. The maximum ultimate load for the pin is 3300 lbs. The pin boundary conditions will be idealized to a simply supported beam for plastic bending analysis, with the reactions placed in between the two cams.

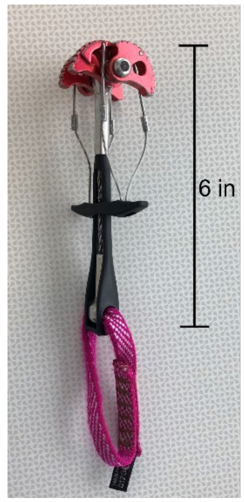

Figure 1.1 Off the Shelf Rock Climbing Cam

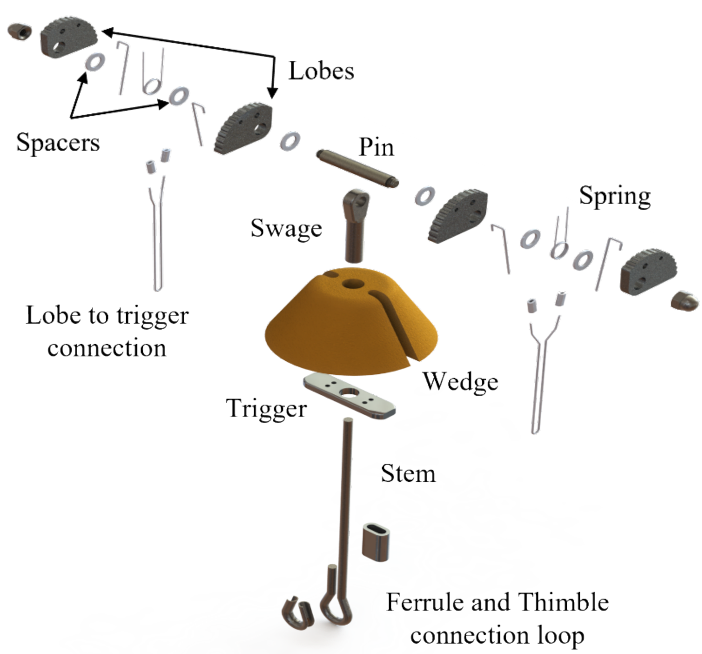

Figure 1.2 Exploded Assembly View of Cam from Senior Design Prototype

There were five members in my senior design team. Muid Khan was the team captain and took charge of delegating tasks and communicating with the client and creating machine drawings. Andrew McConnell performed the boat wave calculations and the testing methods. Jonathan Kroll helped source components, design the testing rig and assemble the prototypes. Mostapha Khazem designed the testing rig and assembly of prototypes. I worked on material selection, pin analysis, and prototype assembly.

1.3 Scope of Honors Work

This honors project expands upon my regular contributions to the senior design effort through an in-depth analysis of the pin as a key load-bearing component. This analysis was carried out using two methods: the Cozzone method and the non-linear finite element analysis (FEA). The pin is modeled with three-point bending boundary conditions. The Cozzone method employs an analytical method to solve for the plastic moment by assuming a trapezoidal stress distribution in the cross-section of the pin. The non-linear FEA model uses the entire stress-strain curve to analyze the nodal elements. These methods are compared to the elastic method and experimental results.

CHAPTER 2

LITERATURE REVIEW

2.1 Elastic Bending

Elastic bending theory is used when a material is loaded below the proportional limit on the stress-strain curve. The stress at the neutral axis is assumed to be zero since each section plane remains in plane after bending. Therefore, the stress distribution of elastic bending is linear from the neutral axis to the outer fiber, and the greatest stress is on the outermost fiber (Cozzone, 1943, pp. 137-139). The stress distribution is shown in Figure 2.1.

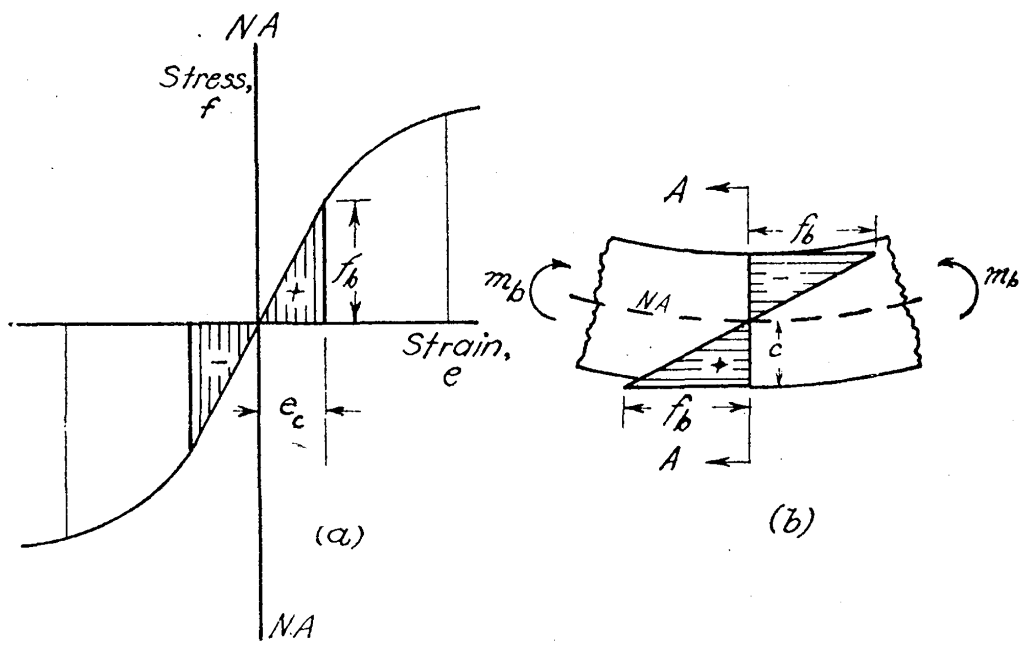

Figure 2.1. Linear Stress Distribution

The equation that governs the bending stress in a section is the conventional formula:

$$f_b = \frac{Mc}{I} \tag{1}$$

Additionally, one side of the section will be in tension and the other side will be in compression. For even materials, the stress distribution is the same since the material behaves the same in tension and compression (Cozzone, 1943, pp. 137-139).

2.2 Plastic Bending and Cozzone Method

Plastic bending occurs when the material is loaded past the elastic zone and begins to strain harden. The stress distribution of the cross section follows the stress-strain curve, which is no longer linear. Modeling this distribution becomes much more complex. Figure 2.2 shows how the stress distribution follows the stress-strain curve. The total resisting moment can be calculated by equation (2).

$$m_r = 2f_rQ_m \tag{2}$$

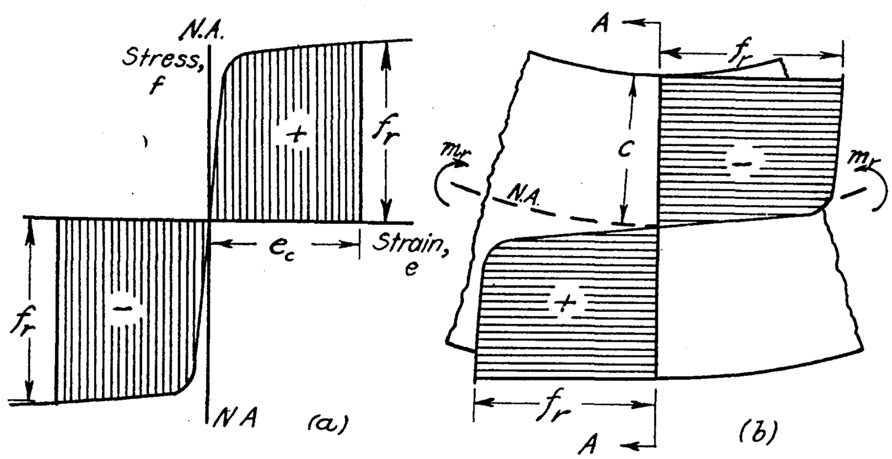

Figure 2.2 Non-linear Stress Distribution

The Cozzone method modifies this stress-strain curve by assuming a trapezoidal stress-strain distribution. This distribution can be visualized in Figure 2.3. The Cozzone method can only be used with materials that have even properties (Cozzone, 1943, pp. 139-140).

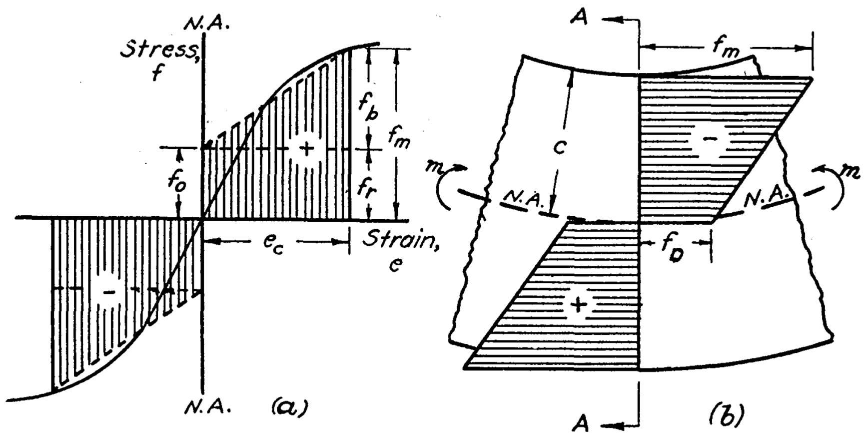

Figure 2.3. Trapezoidal Stress Distribution

The resisting moments can be rewritten as follows:

$$m = m_b + m_r \tag{3}$$

The resisting moments m_b and m_r are substituted in equation (4).

$$m = f_b\left(\frac{I}{c}\right) + 2f_r Q_m \tag{4}$$

By equating $f_r = f_o$ and substituting $f_b = f_m - f_o$ these equations into equation (4) yields equation (5).

$$m = f_m\left(\frac{I}{c}\right) + f_o\left(2Q_m - \frac{I}{c}\right) \tag{5}$$

By regrouping the terms in equation (5), the equation reduces to equation (6).

$$\frac{mc}{I} = f_m + f_o\left(\left(\frac{2Q_m}{I/_c}\right) - 1\right) \tag{6}$$

The term k will be defined in equation (7).

$$k = \frac{2Q_m}{I/_c} \tag{7}$$

The final equation reduces to equation (8).

$$f_b = f_m + f_o(k - 1) \tag{8}$$

2.3 Defining f_o

The stress at the neutral axis f_o needs to be calculated for different materials. In the paper by Cozzone (1943), there are ways to derive f_o with different cross-sections and materials (pp. 149-151). In the book, *Analysis and Design of Flight Vehicle Structures* by E. F. Bruhn (1973), there are some f_o properties for different materials (pp. C3.5-C3.6). However, the list of materials with f_o is not extensive. The equation for f_o can be found from the online book *Analysis and Design of Composite and Metallic Flight Vehicle Structures* (2019, p. 170).

$$\frac{f_0}{f_m} = \frac{6}{{e_u}^2} \cdot \left[\frac{1}{3} \cdot \left(\frac{f_m}{E}\right)^2 + e'_u \cdot \left(\frac{n+1}{n+2}\right) \cdot \left(\frac{{f_m}^{n+1}}{E \cdot {F_{tu}}^n}\right) + \frac{n}{2 \cdot n + 1} \cdot {e'_u}^2 \cdot \left(\frac{f_m}{F_{tu}}\right)^{2n}\right] - 2 \tag{9}$$

Where n- is the Ramsberg-Osgood number.

$$n = \frac{\log\left(\frac{e'_u}{0.002}\right)}{\log\left(\frac{F_{tu}}{F_{ty}}\right)} \tag{10}$$

The plastic strain can be described as

$$e'_u = e_u - \frac{F_{tu}}{E} \tag{11}$$

The total strain is described by the Ramberg-Osgood equation.

$$e_u = \frac{F_{tu}}{E} + 0.002\left(\frac{F_{tu}}{F_y}\right)^n \tag{12}$$

2.4 Material Non-Linear FEA

The multi-linear isotropic stress-strain is an option in ANSYS for plastic analysis. This method allows you to manually type in the values of stress and strain to build a stress-strain curve. The Ramberg-Osgood equation is used to develop these values of stress and strain. The Ramberg-Osgood equation is originally found in technical note No. 902, Description of Stress-Strain Curves by Three Parameters by Walter Ramberg and William R. Osgood (1943, p. 4). The equation adds the elastic strain and plastic strain together for a total strain.

$$\varepsilon = \frac{\sigma}{E} + K\left(\frac{\sigma}{E}\right)^n \tag{13}$$

The MIL-HDBK-5H December 1998 edition shows more examples on how to use the stress-strain curve with a slightly modified equation (p. 9-76).

$$e_{total} = \frac{\sigma}{E} + 0.002\left(\frac{\sigma}{\sigma_y}\right)^n \tag{14}$$

n- is found by using equation (10).

CHAPTER 3

Technical Discussion

3.1 Materials and Setup

The pin under consideration is 3/8" inch diameter and has a length of 2.35 inches (Figure 3.1). The material of the pin is initially selected as 1040 steel. The heat treatment, temper, or properties of the pin are not considered. The assumed material properties of the pin shown in Table 3.1 are from matweb.com for 1040 hot rolled steel.

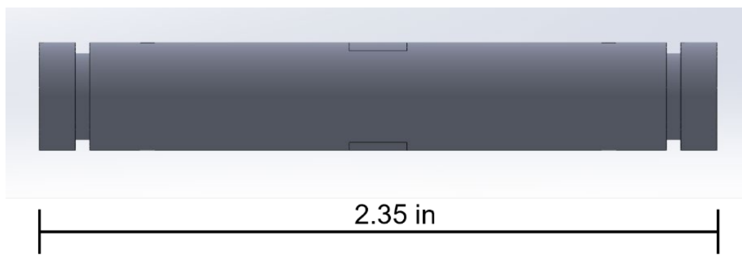

Figure 3.1 Picture of Modeled Pin

Table 3.1. Material Properties for 1040 Hot Rolled Steel

Fut	76	ksi
Fy	42	ksi
E	29000	ksi
v	0.29	
Elongation at break	18%	

The pin is modeled as a simply supported beam as shown in Figure 3.2 with the shear moment diagram of the system.

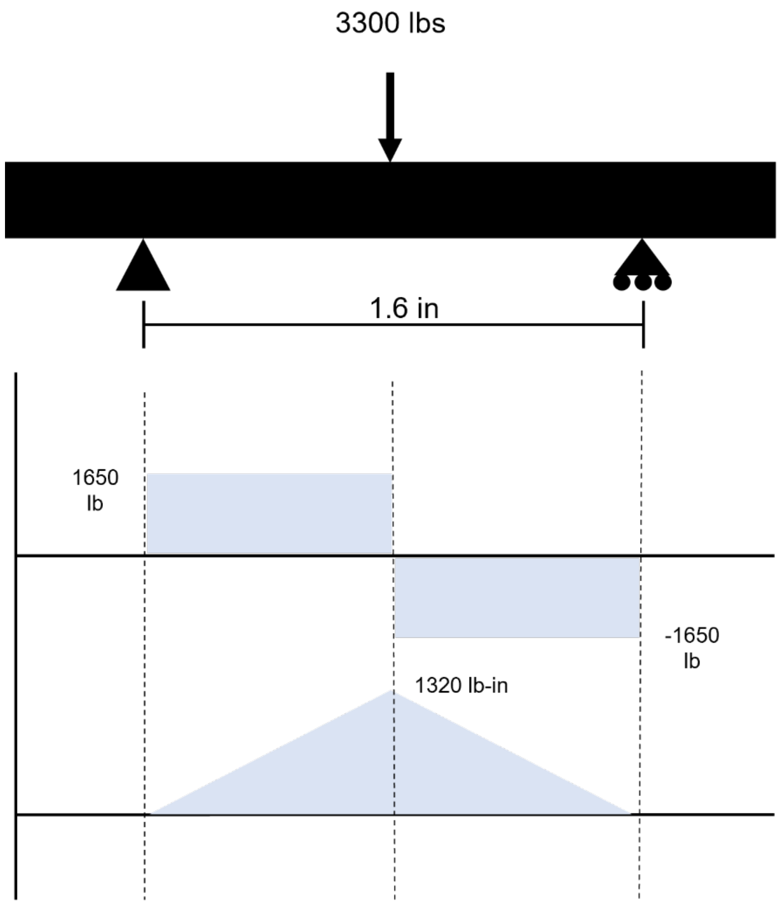

Figure 3.2 Shear Moment Diagram

The maximum moment from the shear moment diagram is 1320 lb-in and the maximum shear is 1650 lb. The moment of inertia for the cross-section is calculated to be 0.00097 in^4. Therefore, using the equation (1) to calculate the bending stress, the maximum bending stress is equal to 255 ksi. The shear strength of the material was calculated at half of the yield strength τ = 21 ksi. The shear stress can be calculated by equation.

$$\tau = \frac{4V}{3A} \tag{15}$$

$$\tau = 20\ ksi$$

The shear stress is below the shear yield strength at the maximum load.

3.2 Cozzone Method

The stress in the neutral axis f_o was calculated using equation (9). The MatLab code used for the Cozzone method is in the appendix. For a solid circular cross-section k =1.7 and $f_m = F_{ut}$ (Bruhn, 1973, p. C3.3).

$$f_b = f_m + f_o(k - 1) \tag{8}$$

$$f_b = 119 \text{ ksi}$$

Solving for the moment.

$$M_{plastic} = \frac{f_b I}{c} \tag{16}$$

$$M_{plastic} = 617 \text{ lb-in}$$

3.2.1 Comparisons

Using the elastic method, the moment is calculated at ultimate strength.

$$M_{Elastic} = \frac{F_{ut} I}{c} \tag{17}$$

$$M_{Elastic} = 390 \text{ lb-in}$$

This moment by elastic calculations is only 63% of the allowable moment of the Cozzone method. However, the maximum moment the pin experiences as shown in the shear-moment diagram is 1320 lb-in. Therefore, the pin will have exceeded the allowable stress set by the Cozzone method and experience failure.

3.3 Multi-Linear Isotropic Plasticity

Stress and strain values were entered into ANSYS from the Ramberg-Osgood equation (10). Figure 3.2 shows this curve.

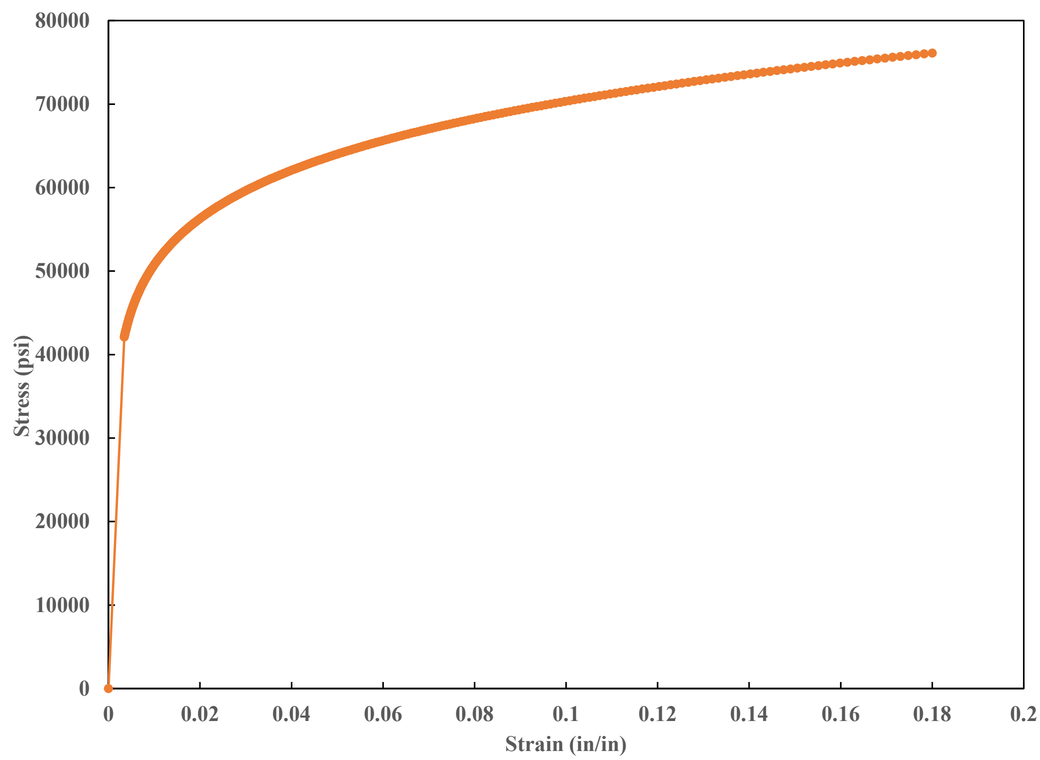

Figure 3.3 Derived Stress-Strain Curve from the Ramberg-Osgood Equation

When running an ANSYS model, the displacement supports were used to prevent rigid body motion. These reactions (ANSYS displacement supports) were assigned to a small square on the bottom of the pin with an area of 0.0025 in^2. The orientation of the pin can be seen in Figure 3.4. The y-axis is parallel to the force, x-axis is parallel to the axial direction, and "z" is coming out of the pin. Displacement supports prevent displacement and prevent moment due to the reaction forces. On one side, constraining x and y creates a pinned support by reacting to the reaction forces. The z-axis is then constrained to prevent rotation. On the opposite side, constraining "y" reacts the vertical reaction force. Constraining the z-axis prevents rotation. The x-axis is free because the surface area selected already constrains rotation about the x-axis.

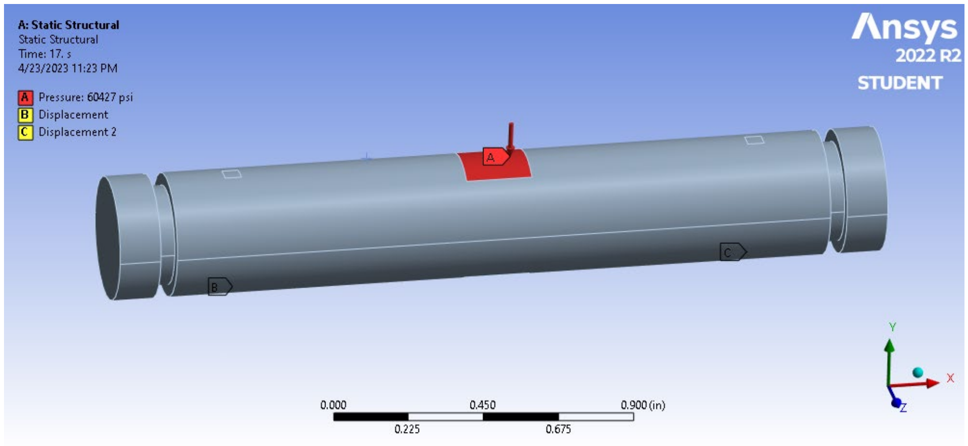

Figure 3.4 Pin Orientation

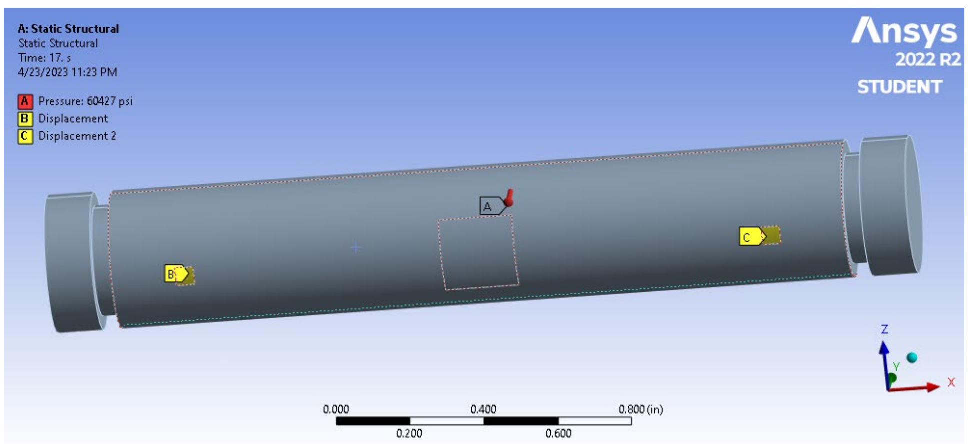

Figure 3.5 Reaction Forces Location

The mesh is auto-generated by ANSYS. The mesh was refined where the force is applied, and where the reactions are applied Figure 3.6-3.7. The force was applied to an area on the pin as a pressure in load steps based on 150 lb increments as shown in Table 3.2. The area is 0.42 in^2 where the pressure is applied.

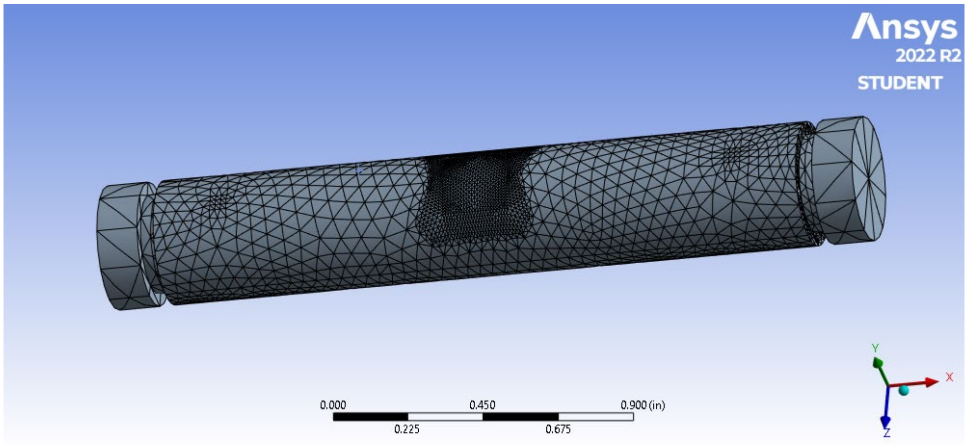

Figure 3.6 Mesh Refinement

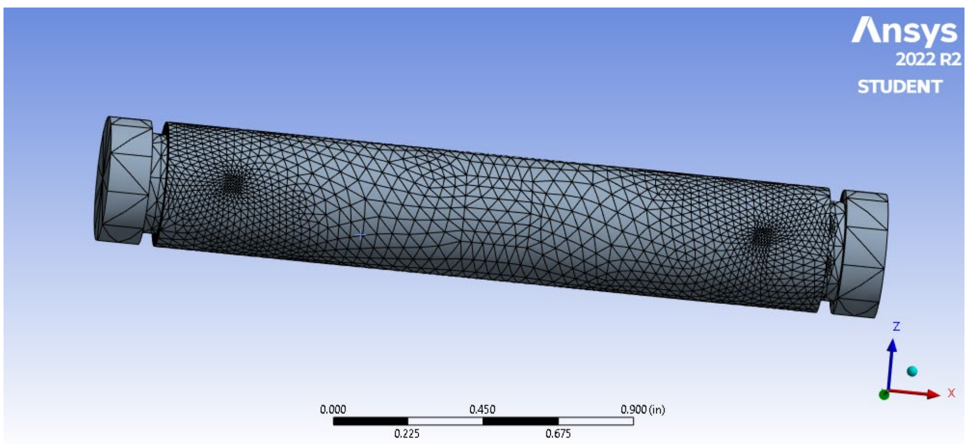

Figure 3.7 Reaction Supports

Table 3.2 Load Step Increments

Load Step	Force (lb)	Pressure (psi)
1	150	3555
2	300	7109
3	450	10664
4	600	14218
5	750	17773
6	900	21327
7	1050	24882
8	1200	28436
9	1350	31991
10	1500	35545
11	1650	39100
12	1800	42654
13	1950	46209
14	2100	49763
15	2250	53318
16	2400	56872
17	2550	60427
18	2700	63981
19	2850	67536
20	3000	71090
21	3150	74645
22	3300	78199

The simulation was then run but was not able to converge to 3300 lbs. because the solution experienced significant elemental distortion at one of the reactions. The simulation iterated through load step fifteen successfully. This level of convergence was enough to determine that the model was not following the experimental data, as the pin would continue to bend in simulation.

There are three items to observe about the results: total deformation, maximum principal stress, and total strain. The total deformation in simulation is the magnitude of all the directions. The maximum principal stress and total strain values in the graphs were values at node 3926. The total strain is the elastic plus the plastic strain. This node was chosen to prevent the maximum reaction stress/strain value from being recorded at the reaction forces. Each result is accompanied with a picture of the deformed pin at load step fifteen and a graph.

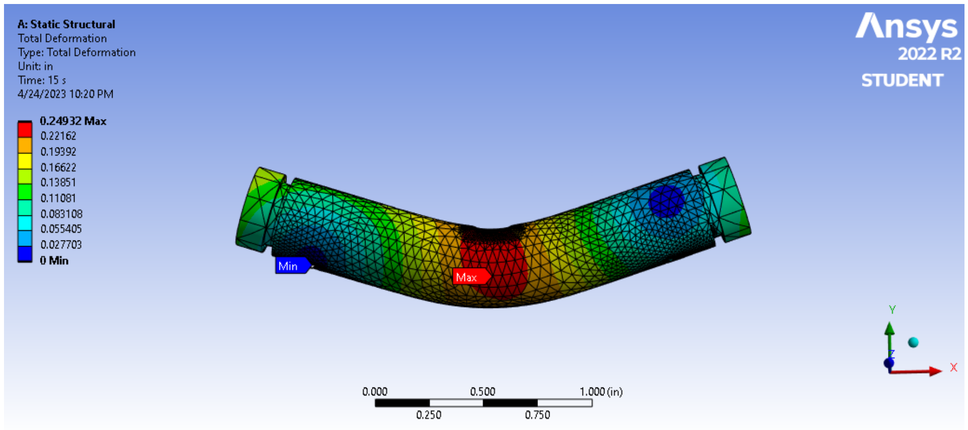

Figure 3.8 Total Deformation

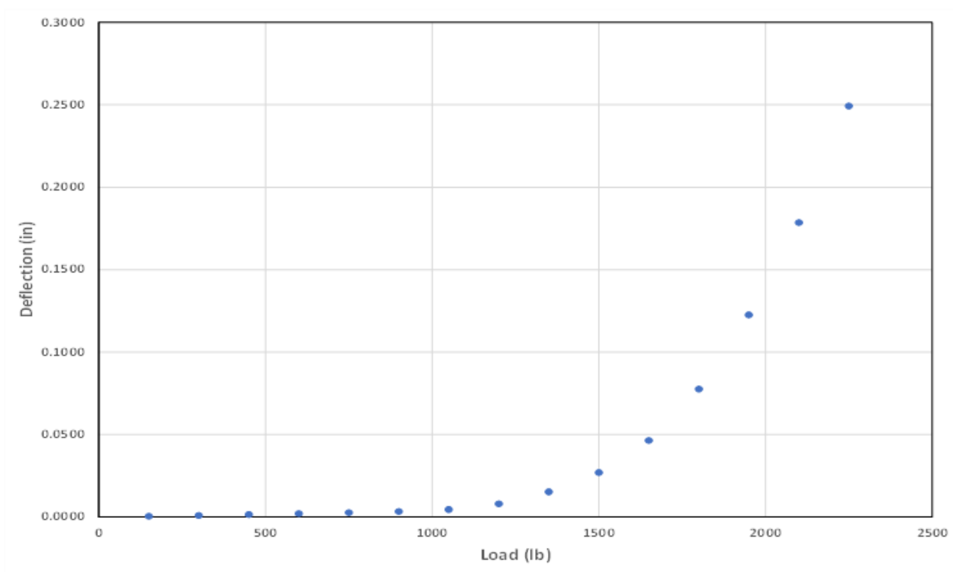

Figure 3.9 Total Deformation Versus Load

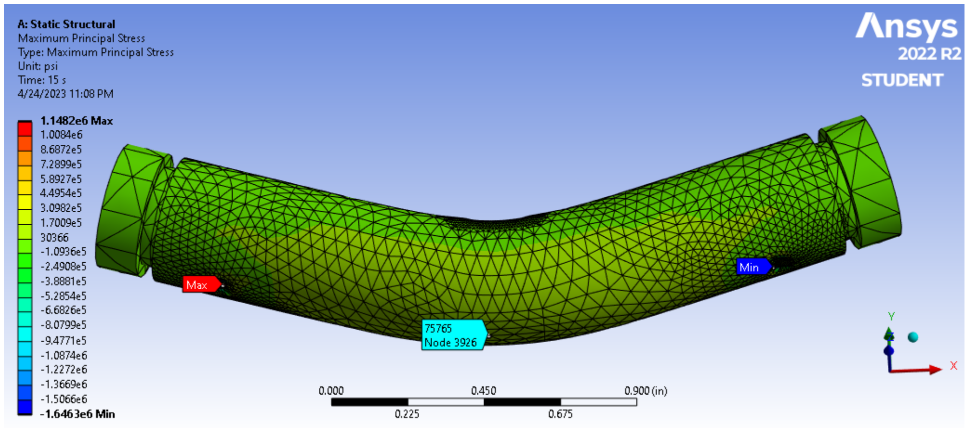

Figure 3.10 Maximum Principal Stress

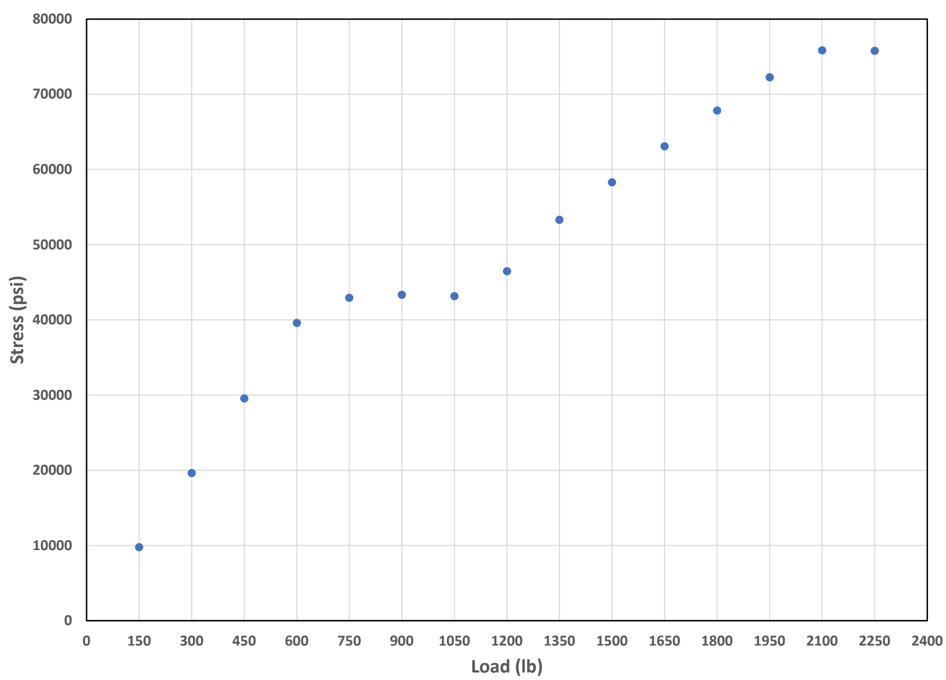

Figure 3.11 Maximum Principal Stress versus Load

The material reaches yield strength at about 600 lb. This analysis was then carried forward in the plastic range.

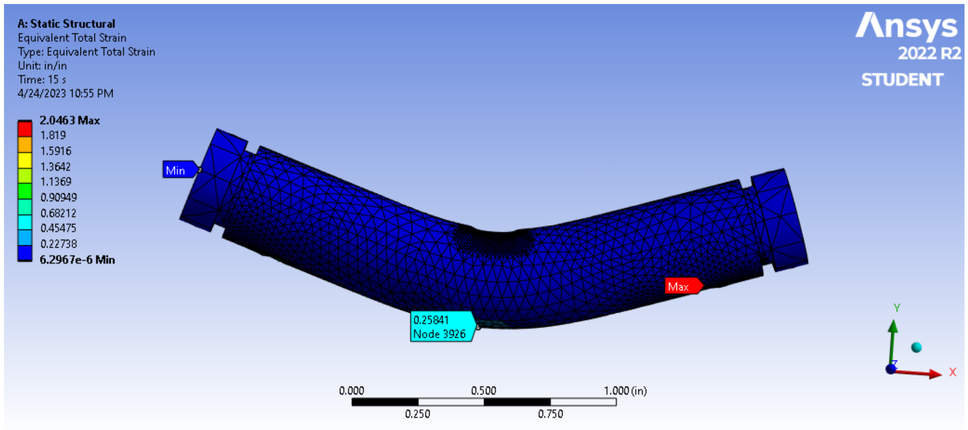

Figure 3.12 Total Strain

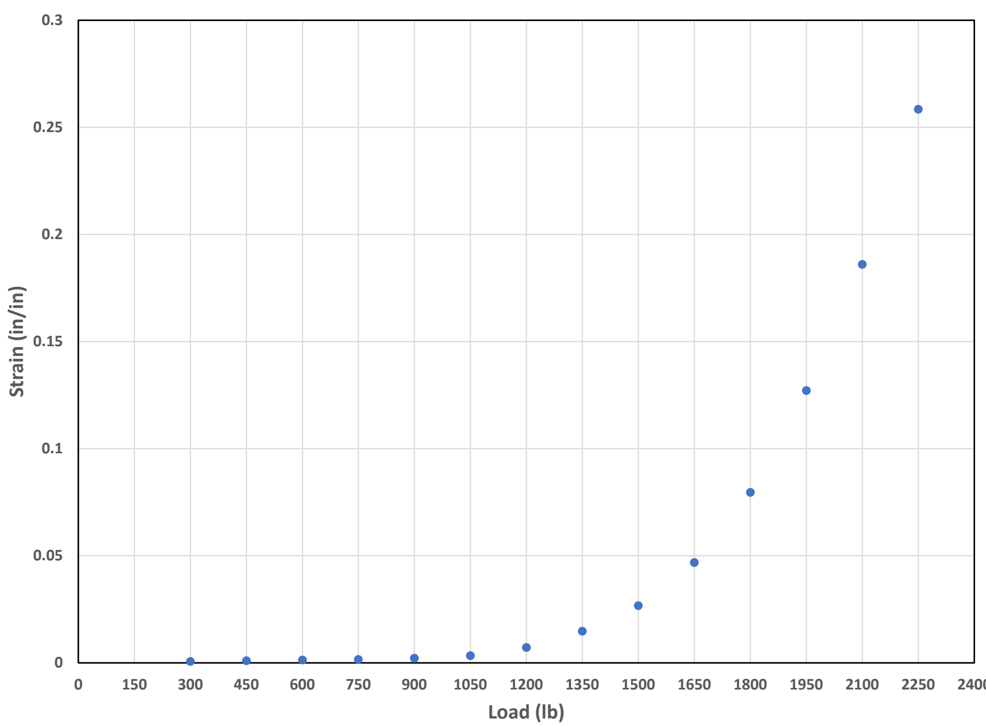

Figure 3.13 Total Strain Versus Load

The strain value at the yield strength of the material is 0.00145 in/in is reached between the load 600 lbs to 750 lbs This means that the material enters the plastic range very quickly.

<u>3.4 Lessons Learned</u>

There are many contributing factors to having a finite element analysis accurately represent actual physical phenomena. There were several errors along the way that need correction including tangential force, elemental distortion, discontinuous mesh, and supports.

The first error to come up in ANSYS was applying the load tangentially to the pin shown in Figure 3.14. This produced a torque on the pin. This was fixed by selecting a single node to ensure the load was applied normal to the surface.

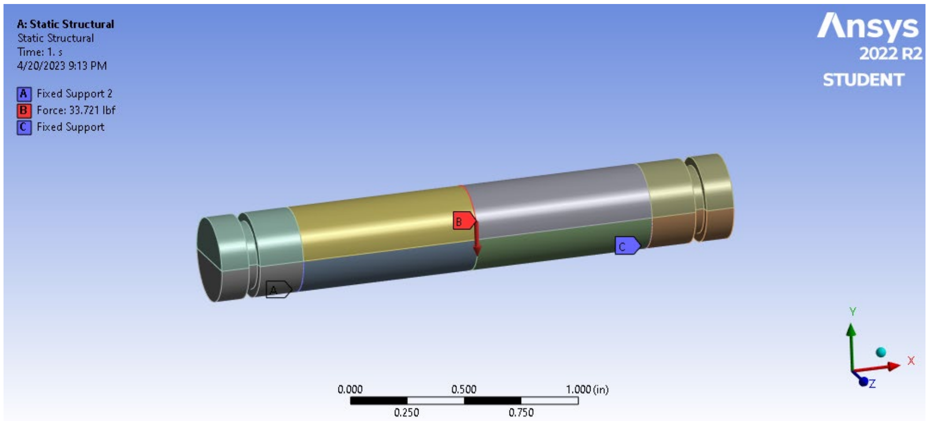

Figure 3.14 Applied Load Error

The next error was elemental distortion when the load was applied to a single node.

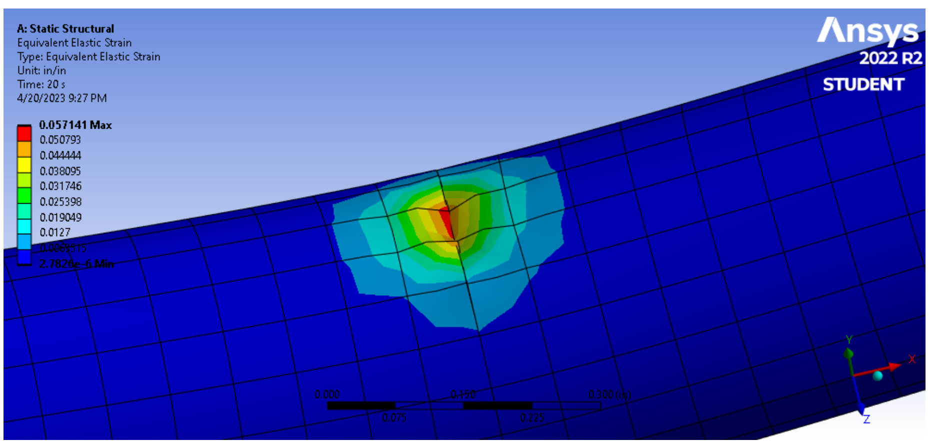

Figure 3.15 Elemental Distortion

The fix for the elemental distortion was to add a small surface at the top of the pin to apply pressure. Refining the mesh is another method to reduce elemental distortion.

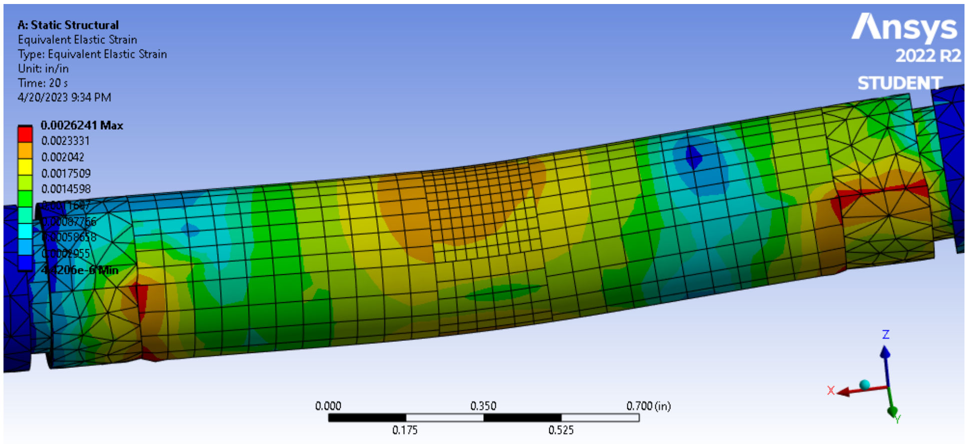

Figure 3.16 Discontinuous Mesh

The solution to the discontinuous mesh was to make sure ANSYS was not treating the surfaces as separate bodies. This was done by reconfiguring the model in SolidWorks with the split and projection tool.

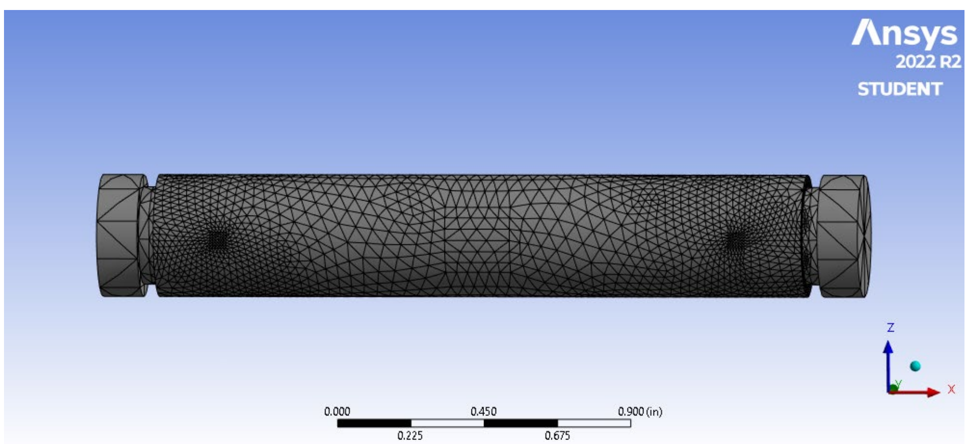

Figure 3.17 Continuous Refined Mesh Side One

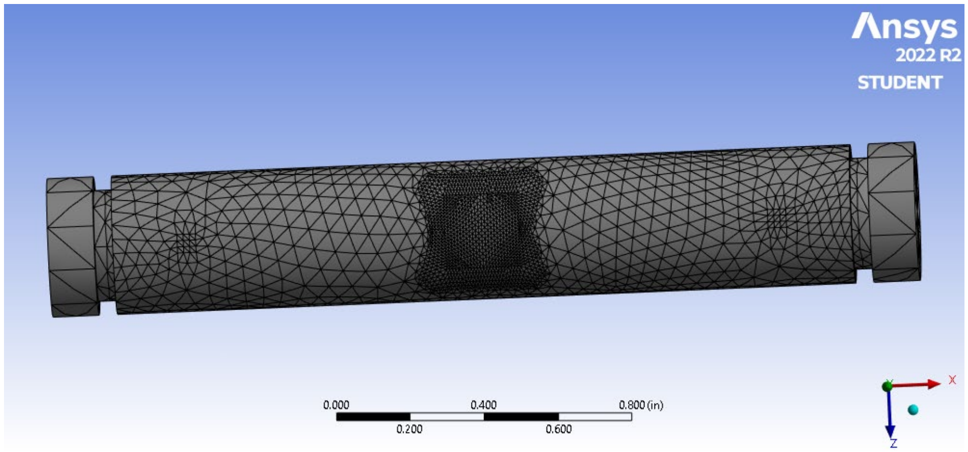

Figure 3.18 Continuous Refined Mesh Side 2

Additionally, how the part is constrained in ANSYS is very important. The goal is to prevent rigid body motion. This means all six degrees of freedom need to be accounted for and constrained. The pin is assumed to be a simply supported beam. This means one side is pinned and the other side is on roller supports. Several different supports were used in ANSYS before the right setup was found. The very first model used fixed supports. These fixed supports are incorrect, because fixed supports constrain all degrees of freedom, allowing no rotation for bending. The correct boundary conditions are two displacement supports. This allowed for a pinned and roller simply supported beam setup.

3.5 Experimental Data

The three-point bending test was conducted on an Instron 8801 tensile testing machine. The deformation rate was 0.05 in/min. The pin was loaded to 3300 lb. Figures 3.19-3.21 show the test setup and results.

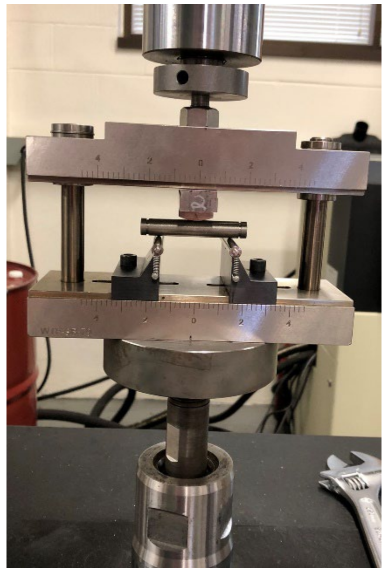

Figure 3.19 Test Setup

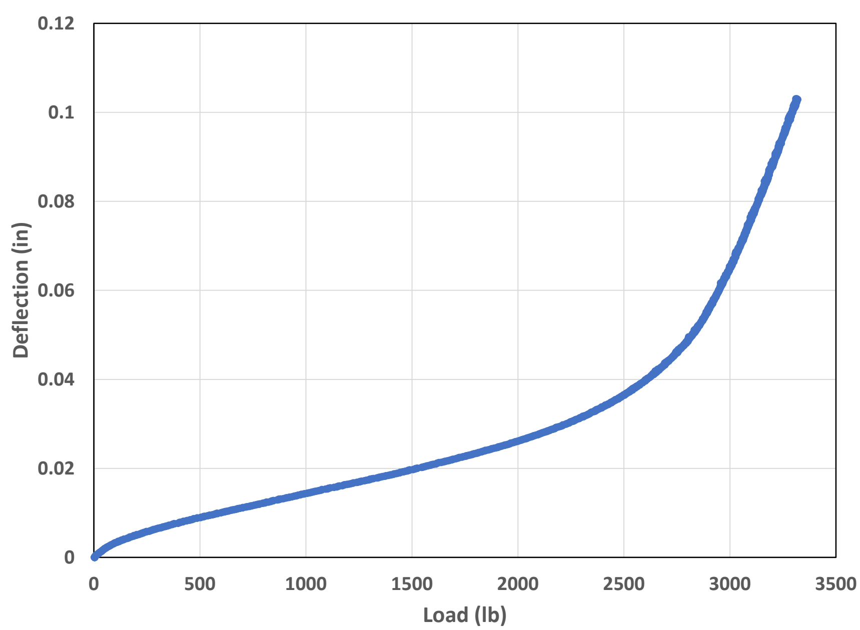

Figure 3.20 Load Versus Deflection

Figure 3.21 Deformed Pin

Figure 3.8 shows the pin has deformed quite significantly, demonstrating the high ductility of the material. This shows the pin will not suddenly rupture, but elongate before fracture.

3.6 Results Comparison

The results of the FEA model did not match the experimental data, as evidenced by Figure 3.22. The deflection of the FEA model increases much more quickly than the experimental data. There are multiple reasons for this discrepancy. The most obvious factor is uncertainty about the material properties. The 1040 steel has a wide range of properties depending on how the stock is processed and heat treated. Additionally, as shown in Figure 3.21 the test material is very ductile. This means that the strain should be cut off at the ultimate strain and not the fracture strain in the Ramberg-Osgood equation. This is another reason for inaccuracies in the model. The Cozzone method clearly shows that 1040 steel will also fail under the maximum loading conditions.

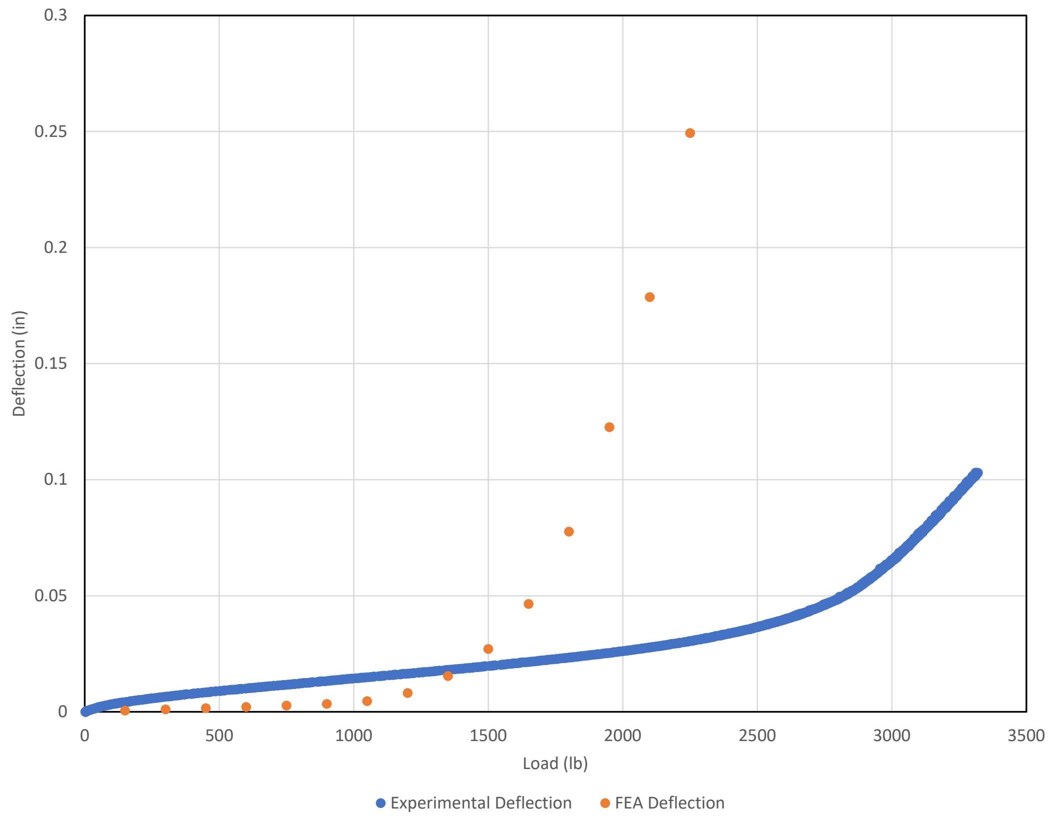

Figure 3.22 Comparing the Deflections

3.7 Alternative material selection

Since 1040 steel resulted in failure, an alternate material was investigated. AM 355 stainless steel with the specification AMS 5743 and condition of SCT850b has the following material properties (MIL-HDBK-5H, 1998, p. 2-124).

Ftu = 200ksi

Fty = 165ksi

Elongation is 10%

Running the Cozzone code again, the Mplastic =1690 lb-in allowable moment. This is above the Mmax = 1320 lb-in. Any material with around a 200 ksi ultimate tensile strength will withstand the maximum load.

CHAPTER 4

CONCLUSIONS

The results of this experiment show the pin failure at a maximum load of 3300 lbs with the current material choice of 1040 steel, assuming hot rolled properties. Both the Cozzone method and the FEA model confirm this result. However, the experimental data did not match the FEA model. This discrepancy is attributed to unknown material properties and the ductility of the 1040 steel. An alternate material choice which could handle this type of load is AM 355 stainless steel. The Cozzone method does demonstrate how much more capability the part has within the plastic range when compared to the elastic bending moment.

CHAPTER 5

FUTURE IMPROVEMENTS

There are several ways to improve this work. First, knowing the exact stress-strain curve from either a data base or in house tensile test of a specimen would ensure accurate data. Additionally, one could improve the ANSYS simulation supports by modeling the roller supports and the pin in the simulation.

APPENDIX A

CODE USED IN PROJECT

Code for 1040 steel.

```
% Honors College Capstone Project
% Cozzones Method for plastic bending

%Material Properties
%1040 hot rolled steel from matweb
Ftu = 76100; %psi
Fy = 42100; %psi
v = 0.29; %piossions ratio
E = 29000000; %psi

%Defining cross-section properties.
Diameter=3/8; %inches
A = pi()*0.25*Diameter^2;
I = (pi()*(3/8)^4)/64; %inches^4
c = 3/16; %inches

%% From shear moment diagram
V=1650; %lb
Mmax = 1320; %lb-in
Sbending = (4*V)/(3*A)

%% Strain at Ultimate and Ramberg-Osgood Shape Factor

% 3 unknowns and 3 eqns
%eu = Ftu/E + 0.002(Ftu/Fy)^(log((eu-Ftu/E)/0.002)/log(Ftu/Fty))  %total
strain at failure elastic
eu = 0.18;  % elongation at break 18% from matweb
ep = eu-Ftu/E;%ep = plastic strain at failure
n=log(ep/0.002)/log(Ftu/Fy); %Ramberg-Osgood shape factor

%% Calculate Fo curve
fo =
(6*Ftu/(eu^2))*((1/3)*((Ftu/E)^2)+ep*((n+1)/(n+2))*((Ftu^(n+1)/(E*Ftu^n)))+((n
/(2*n+1))*(ep^2)*(Ftu/Ftu)^(2*n)))-2*Ftu

%% Calculating moments and Fb

%Mb = total internal resisting moment
%mr = internal moment developed by portion r
%mb = internal moment developed by protion b

%Mb = mr + mb

%mr = fo2Q
%mb = fbI/c

% k = 2Q/(I/c)
```

```
%Mb = (fm - fo)(I/c)+2foQ

%Fb = fm +fo(k-1)

%calculate the shape factor
%k=2Q/(I/c)
Q = ((c*2)^3)/12;
k= (2*Q)/(I/c)

Fb = Ftu +fo*(k-1)

Mult = Fb*I/c

>> CozzoneCode

Sbending =

   1.9919e+04


fo =

   6.1674e+04


k =

    1.6977


Fb =

   1.1913e+05


Mult =

  616.7422
```

Code for AMS Stainless Steel

```
% Honors College Capstone Project
% Cozzones Method for plastic bending

%Material Properties
%AM 355 Stainless Steel From mil HDBK 1998 - p178
Ftu = 200000; %psi
Fy = 165000; %psi
v = 0.29; %piossions ratio
```

```
E = 29000000; %psi

%Defining cross-section properties.
Diameter=3/8; %inches
A = pi()*0.25*Diameter^2;
I = (pi()*(3/8)^4)/64; %inches^4
c = 3/16; %inches

%% From shear moment diagram
V=1650; %lb
Mmax = 1320; %lb-in
Sbending = (4*V)/(3*A)

%% Strain at Ultimate and Ramberg-Osgood Shape Factor

% 3 unknowns and 3 eqns
%eu = Ftu/E + 0.002(Ftu/Fy)^(log((eu-Ftu/E)/0.002)/log(Ftu/Fty))  %total
strain at failure elastic
eu = 0.10;  % elongation at break
ep = eu-Ftu/E;%ep = plastic strain at failure
n=log(ep/0.002)/log(Ftu/Fy); %Ramberg-Osgood shape factor

%% Calculate Fo curve
fo =
(6*Ftu/(eu^2))*((1/3)*((Ftu/E)^2)+ep*((n+1)/(n+2))*((Ftu^(n+1)/(E*Ftu^n)))+((n
/(2*n+1))*(ep^2)*(Ftu/Ftu)^(2*n)))-2*Ftu

%% Calculating moments and Fb

%Mb = total internal resisting moment
%mr = internal moment developed by portion r
%mb = internal moment developed by portion b

%Mb = mr + mb

%mr = fo2Q
%mb = fbI/c

% k = 2Q/(I/c)

%Mb = (fm - fo)(I/c)+2foQ

%Fb = fm +fo(k-1)

%calculate the shape factor
%k=2Q/(I/c)
Q = ((c*2)^3)/12;
k= (2*Q)/(I/c)
```

```
Fb = Ftu +fo*(k-1)

Mplastic = Fb*I/c
Melastic = Ftu*I/c

>> Cozzone2

Sbending =

   1.9919e+04


fo =

   1.8283e+05


k = 1.6977


Fb =

   3.2755e+05


Mplastic =

   1.6958e+03


Melastic =

   1.0354e+03
```

REFERENCES

Abbott, Richard. (2019). *Analysis and Design of Composite and Metallic Flight Vehicle Structures.* Abbott Aerospace. https://www.abbottaerospace.com/downloads/analysis-and-design/

Bruhn, E. F., (1973). *Analysis and Design of Flight Vehicle Structures.* Jacobs Publishing.

Cozzone, Frank P. (1943). *Bending Strength in the Plastic Range. Journal of The Aeronautical Sciences, 10*(5), 138-151. 10.2514/8.11021

Department of Defense. (1998). *Military Handbook: Metallic Materials and Elements for Aerospace Vehicle Structures.* Abbott Aerospace. https://www.abbottaerospace.com/downloads/mil-hdbk-5h-metallic-materials-and-elements-for-aerospace-vehicle-structures/

MatWeb: Material Property Data, *AISI 1040 Steel Hot Rolled*, https://matweb.com/search/DataSheet.aspx?MatGUID=81926101a0254bd6a0a6797e190c6877&ckck=1

Osgood, William R., Ramberg, Walter. (1943). Description of Stress-Strain Curves by Three Parameters. Technical Note 902. *National Advisory Committee for Aeronautics.* https://www.abbottaerospace.com/downloads/naca-tn-902-description-of-stress-strain-curve-by-three-parameters-ramberg-osgood/

BIOGRAPHICAL INFORMATION

Mikaela Leevy will graduate on May 12, 2023, from The University of Texas at Arlington with an Honors Bachelor of Science in Mechanical Engineering.

While at UTA, Mikaela was a Peer Academic Leader for three semesters and a member of the Society of Manufacturing Engineers.

Upon graduation, Mikaela will participate in an internship with the Airforce at the Wright-Patterson Airforce Base in Dayton, Ohio. In the fall, Mikaela will continue her education here at The University of Texas at Arlington Mechanical Engineering graduate program.